

# Pattern design and realization for calibrating near infrared camera in surgical navigation\*

WEN Xiao-yan (温小艳), LIU Su-juan (刘素娟), YANG Rong-qian (杨荣骞)\*\*, and WANG Zhi-gang (王志刚)  
 Department of Biomedical Engineering, South China University of Technology, Guangzhou 510006, China

(Received 25 April 2012)

©Tianjin University of Technology and Springer-Verlag Berlin Heidelberg 2012

A calibration board composed of  $8 \times 8$  near-infrared surface-mounted diodes (NIR-SMDs) (940 nm) is designed. Meanwhile, a common binocular measurement system with the average error less than 0.1320 mm is used to obtain the geometric information of this board. A calibration method with the designed pattern is performed to obtain the parameters of the near-infrared camera (NIRC). In the experiment, the average relative errors of focal length and principal point are 0.244% and 0.735%, respectively. The mean of image residuals is less than 0.01 pixel. The error of three-dimensional (3D) measurement is less than 0.3 mm. All those results indicate that the designed calibration board is suitable and accurate for calibrating NIRC.

**Document code:** A **Article ID:** 1673-1905(2012)06-0409-5

**DOI** 10.1007/s11801-012-2265-y

The near-infrared camera (NIRC) in surgical navigation is composed of a visible camera and a near-infrared filter, and it needs to be calibrated to realize positioning. So it's important to calibrate the NIRC accurately with a suitable calibration board and the corresponding method.

The camera calibration methods for visible camera are classified into two categories of traditional calibration and self-calibration<sup>[1,2]</sup>. In the progress of calibration based on pattern, many calibration methods are based on two stages<sup>[3-6]</sup>, including direct linear transformation (DLT) and nonlinear optimization<sup>[7,8]</sup>, in which Zhang's method is more flexible and practical using mobile pattern<sup>[5]</sup>. There are two solutions<sup>[1]</sup> for the pattern used in above methods which can't be sensed by NIRC. One is that the calibration results of NIRC are obtained from the camera without filter, and the other is that an external light source is introduced to make the camera sense the calibration board such as checkerboard. However, the former cannot meet the need of the calibration accuracy, and the latter will introduce the reflected light from the surroundings.

For the purpose of directly calibrating NIRC, a calibration board with 64 ( $8 \times 8$ ) near-infrared surface-mounted diodes (NIR-SMDs) is designed. The three-dimensional (3D) coordinates of the light-emitting points are measured by an accurate visible binocular vision system in darkroom, and

then a series of transformations are used to obtain a calibration pattern which is independent of the measurement system and can be used to calibrate the NIRC directly. In this paper, the existing calibration methods and the designed pattern are used to calibrate the NIRC to obtain the internal and external parameters. Further, the image residuals and the error of the 3D measurement are employed to verify the accuracy of the pattern and the calibration results of NIRC.

The geometric information of the calibration board is very important for accurate calibration<sup>[4]</sup>. The board in Fig. 1(a) is impossible to be used directly for calibrating NIRC because its geometric information is unknown. Therefore, a binocular vision system composed of two visible cameras is designed to obtain this information. The optical spectrum of the charge coupled device in the visible camera covers near-infrared wavelength. The binocular vision system is calibrated to obtain the model parameters of  $A_l, A_r, k_l, k_r, R_{lr}, T_{lr}, R_{lg}, T_{lg}, R_{rg}$  and  $T_{rg}$  in our previous work<sup>[9]</sup>, where  $A_l$  and  $A_r$  are the internal parameters,  $k_l$  and  $k_r$  are distortion factors.  $S_l$  and  $S_r$  are used for left and right camera coordinate systems, respectively, and  $S_g$  is for the global coordinate system of this binocular vision system. So  $R_{lr}$  and  $T_{lr}$  are the rotation matrix and translation vector between  $S_l$  and  $S_r$ , and  $R_{lg}$  and  $T_{lg}$  are those between  $S_l$  and  $S_g$ .

Assuming  $p_g$  as a point in  $S_g$ , its two-dimensional (2D)

\* This work has been supported by the National Natural Science Foundation of China (No. 81101130), the Fundamental Research Funds for Central Universities under the South China University of Technology (No.2012ZZ0095), and the Science and Technology Program of Guangdong Province (No.2012B031800026).

\*\* E-mail: bmeyrq@gmail.com

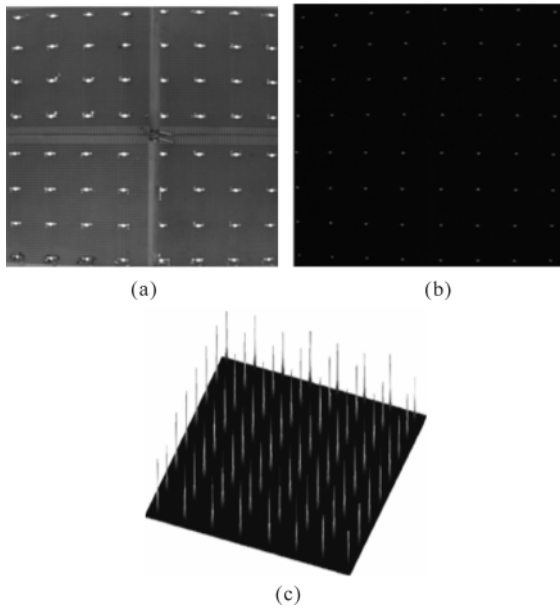


**Fig.1 Calibration boards (a) captured by the visible camera and (b) captured by NIRC, and (c) 3D display of (b) by taking its gray value as altitude**

coordinates on the left and right images captured by the visible binocular stereo vision system are  $p_l=[u_l, v_l]^T$  and  $p_r=[u_r, v_r]^T$ . In  $S_p$ , the normalized coordinate of  $p_l$  is  $p_l'=[u_l, v_l, 1]^T$ . Its light vector is  $v_{pl}=\lambda_l A_l^{-1} p_l'$ , where  $\lambda_l$  is an arbitrary amount, and  $A_l$  stands for the internal parameters of left camera. Similarly, the light vector  $v_{pr}$  is also obtained. Converting  $v_{pl}$  and  $v_{pr}$  into  $S_g$ , we can get linear equations:

$$\begin{cases} \hat{p}_l = R_{lg} v_{pl} + T_{lg} \\ \hat{p}_r = R_{rg} v_{pr} + T_{rg} \end{cases} \quad (1)$$

Let  $\hat{p}_l = \hat{p}_r$ , so their intersection coordinates can be calculated, which are the 3D coordinates of  $p_g$ . During this process, it is necessary to obtain the 2D coordinate values of the light-emitting points on the left and right images accurately, which are named as subpixel coordinates. To avoid the interference from environmental light when extracting the subpixel coordinates, the experiments are carried out in a darkroom, so one of the images for calibration can be obtained as shown in Fig.1(a) and (c). Based on the imaging consistency of the near-infrared markers, the method of gray weighted mean<sup>[10]</sup> is employed to extract the subpixel coordinates.

For an image, four initial values of light spots are obtained by clicking the corresponding points on the four corners in Fig.2. The subpixel coordinate values are calculated using the method of gray weighted mean and are expressed using matrix  $P$  as

$$\square P = \begin{bmatrix} p_{1x} & p_{2x} & p_{3x} & p_{4x} \\ p_{1y} & p_{2y} & p_{3y} & p_{4y} \\ 1 & 1 & 1 & 1 \end{bmatrix}, \quad (2)$$

where  $p_{ix}$  and  $p_{iy}$  ( $i=1,2,3,4$ ) stand for the subpixel coordinate values of the  $i$ -th corner clockwise. In order to facilitate the calculation, a grid matrix of

$$G = \begin{bmatrix} 0 & 1 & 0 & 1 \\ 0 & 0 & 1 & 1 \\ 1 & 1 & 1 & 1 \end{bmatrix} \quad (3)$$

is introduced, so the homography matrix can be obtained as  $H=PG^{-1}$ .

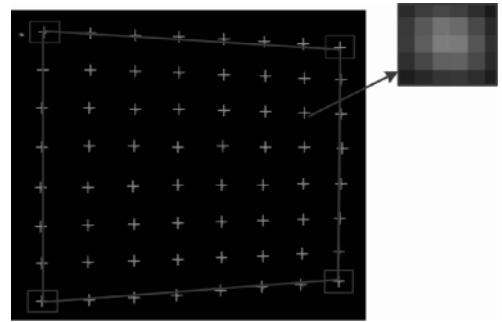


**Fig.2 Subpixel extraction results where “+” represents the positions of the subpixel coordinates**

Let  $F=[0,1,1,1,1,1,1,1]$  and  $D=[1,1,1,1,1,1,1,1]$ , so the grid matrices  $G_x$  and  $G_y$  stand for the horizontal and vertical directions, respectively, which can be obtained as:

$$\begin{cases} G_x = F^T \cdot D/n \\ G_y = D^T \cdot F/n \end{cases}, \quad (4)$$

where  $n=8$  in this paper. For the markers in the  $j$ -th column of image, the corresponding pixel grid is  $G_j=[G_x(j), G_y(j), D^T]^T$ , and the initial value matrix is  $X_j=HG_j^T$ . Thus, the initial coordinates of each light point can be obtained. Then each subpixel coordinate values can be calculated accurately using the method of gray weighted mean. In summary,  $P_i$  ( $64 \times 3$ ) stands for a collection of coordinate values for the  $i$ -th perspective and its values are obtained using Eqs.(1)–(4).

The coordinate values obtained by Eq.(1) depend on the measurement system which can result in measurement error. Based on this, it is necessary to acquire a calibration pattern which is independent of the system. So a series of transformations are used for getting this pattern.

Firstly, let  $P_k$  be the 3D coordinates of 64 points in the  $k$ -th position. Select 64 points  $P_i$  in a position  $P_j$  can be rotated and translated to  $P_i$ , and the two point sets satisfy the following relationship:

$$P_i = R_{ji} \cdot P_j + T_{ji}, \quad (5)$$

where  $R_{ji}$  is a  $3 \times 3$  rotation matrix, and  $T_{ji}$  is a  $3 \times 1$  translation vector. Using the method in Ref.[11],  $R_{ji}$  and  $T_{ji}$  can be

obtained, and then  $P_i$  can be transformed to the position of  $P_j$  to form  $P_j'$  by Eq.(5).

Secondly, according to above,  $P_k$  can be rotated and translated into the position of  $P_i'$ . Regard  $P_i'$  as an initial template, and transform the other positions to  $P_i'$  to get a new sets of points  $P_m$  as a new template. Due to the measurement error, these luminous points on the calibration are not coincident. To enhance accuracy, the mean values of these points are regarded as the real position of the template. And then a new template with 64 points is obtained. Therefore, this new template is used as initial template to repeat the procedure mentioned above until the difference between the new template and the initial template is less than the accepted threshold. The final result of  $P_i'$  is regarded as the geometric information of the calibration board.

Lastly, template  $P_i'$  belongs to the binocular vision coordinate system, and it cannot be used for directly calibrating other camera such as NIRC. Therefore, in a grid coordinate system of  $(X_g, Y_g, Z_g)$ , the coordinate system of calibration board is developed. Its origin is attached to the mean value of  $P_i'$ , and two points  $p_x$  and  $p_y$  in  $P_i'$  are selected to construct a plane  $X_g O_g Y_g$  with the origin. The  $X_g$  axis is aligned with the direction from the origin to  $p_x$ .  $Y_g$  axis coincides with the direction perpendicular to the  $X_g$  axis, and lies on the plane  $X_g O_g Y_g$ . The  $Z_g$  axis is determined by the right-hand rule. Then the template  $P_i'$  can be rotated and translated to the grid coordinate system to form  $P_i$ , which is the calibration pattern for NIRC and independent of the measurement system.

To calibrate the NIRC, it is required to capture a series of images of the designed calibration board. Each subpixel coordinate of the light spots in the images can be extracted accurately as shown in Fig.2. Then the corresponding relationship between the 2D coordinates  $[u_i, v_i]^T$  and 3D coordinates  $[X_i, Y_i, Z_i]^T$  at the  $i$ -th location of the pattern is obtained using the following equation

$$\lambda [u_i, v_i, 1]^T = A [R, T] [X_i, Y_i, Z_i, 1]^T, \quad (6)$$

where  $\lambda$  is an arbitrary scale factor, and  $A$  is an intrinsic parameter matrix of NIRC.  $R$  and  $T$  are extrinsic parameters. According to DLT<sup>[10]</sup>, the parameters  $A$ ,  $R$  and  $T$  are obtained if the number of markers on near-infrared calibration board is greater than or equal to 6. These values of the parameters are regarded as initial parameters in nonlinear optimization for enhancing the accuracy of calibration. So a distortion model<sup>[12,13]</sup> is introduced to get more accurate calibration results, and the Levenberg-Marquardt (LM) algorithm<sup>[13]</sup> is then employed to optimize the intrinsic and extrinsic parameters  $A$ ,  $R$  and  $T$  which can be regarded as the final results of NIRC calibration.

To avoid the interference of environmental light, the ex-

periments are performed in a darkroom. The calibration board is placed in different positions in the field of view of this binocular vision system to obtain  $N$  image pairs, as shown in Fig.1(b). All light spots on these image pairs are extracted<sup>[10]</sup>. Then  $64 \times N$  coordinates of luminous points on the board can be calculated. In experiment,  $N=18$ , and the reconstruction of those 3D coordinates is shown in Fig.3.

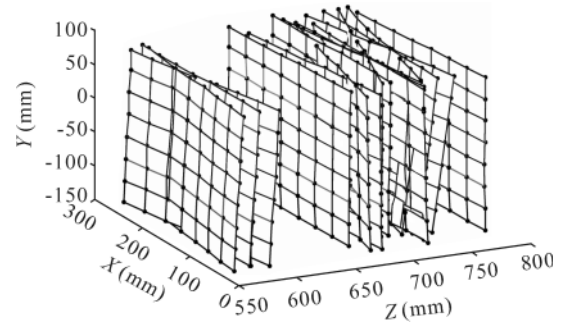
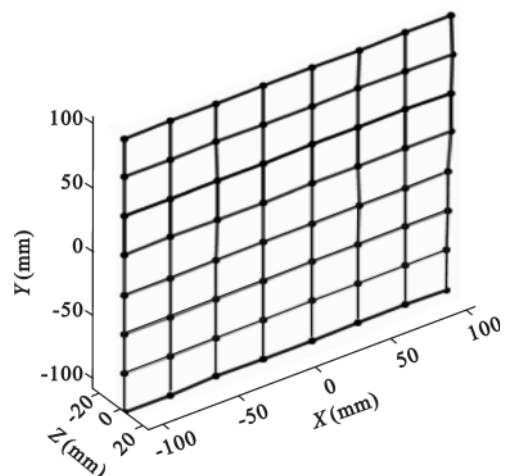


**Fig.3 Reconstruction results of the 3D coordinates at different positions**

With the method described above, the calibration pattern  $P_i$ , which is independent of the measurement system and can be used for calibrating NIRC directly, is obtained and is shown in Fig.4(a). To analyze the precision of this pattern, all 1152 measurement errors are calculated and mapped in Fig.4(b). The mean error is 0.0524 mm, and it meets the accuracy requirement of geometric information for calibration.

16 images are captured with different positions to calibrate the NIRC. Using the method described above, the intrinsic parameters of NIRC are calculated, where the focal length is  $(2055.8815 \pm 4.9406 \text{ mm}, 2054.0412 \pm 5.0810 \text{ mm})$  and the principal point is  $(629.9496 \pm 4.6342 \text{ pixels}, 575.0298 \pm 4.2192 \text{ pixels})$ . The mean relative errors of the focal length and principal point are 0.24% and 0.74%, respectively, and those using the calibration methods in Refs.[6], [13] and [14] for visible cameras are shown in Tab.1.



(a)

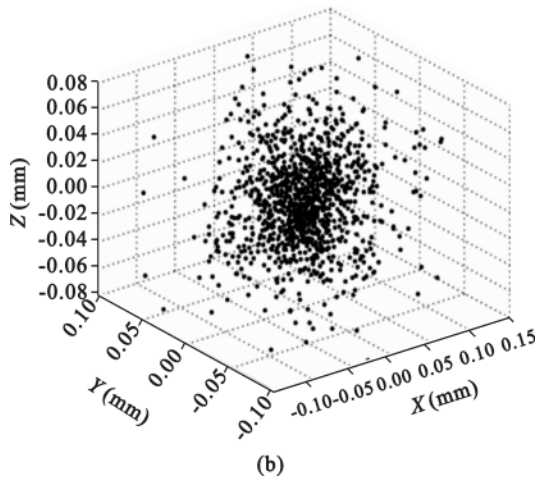


**Fig.4 (a) Template and (b) distribution of the measurement error**

**Tab.1 Mean relative errors**

	Ref.[6]	Ref.[13]	Ref.[14]	Proposal
Focal length	6.82%	0.57%	6.22%	0.24%
Principal point	4.44%	1.20%	0.56%	0.74%

16 images of calibration board obtained by the NIRC can contain 1024 re-projection coordinates, while 1024 residuals are acquired in total and shown in Fig.5. The residuals of X direction mainly concentrate in the interval of -0.6 – 0.6 pixel, in which the number of feature points is 980, accounting for 95.7% of the total, and 944 feature points in the range of -0.5 – 0.5 pixel (92.2%) of Y direction. It means that using the imaging geometry model established by the calibration results is able to describe the NIRC projection process correctly.

A near-infrared binocular vision system is designed to measure the distance between two NIR-SMDs. The real value of the distance is  $36.6886 \pm 0.0186$  mm with relative error of 0.05%. Firstly, the internal and external parameters of the two NIRCs are obtained using the calibration board and the corresponding method described above, and then the relationships among different coordinate systems are obtained

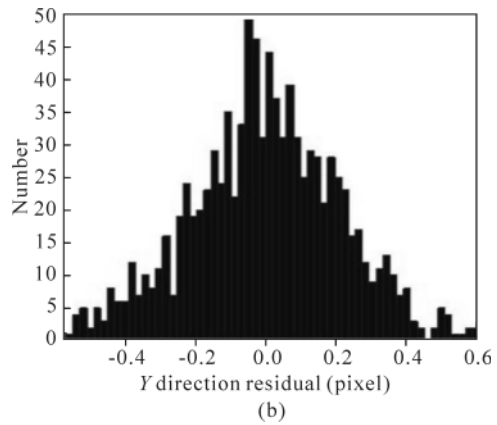
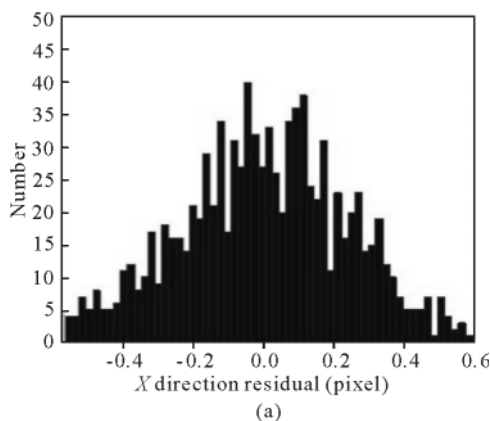


**Fig.5 (a) X direction and (b) Y direction residuals of images**

with the method in our previous work<sup>[11,15]</sup>. Finally, the 3D coordinates of the two points are achieved, and the distances between them at different positions are computed. The error between the measured and the real values is shown in Fig.6. The mean error is 0.0304 mm, and the relative error is 0.08%. In summary, the measured values are close to the real ones, which also indicates that the calibration board and the used method are effective.

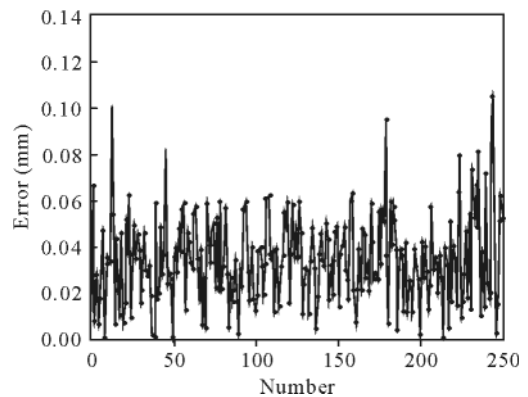


**Fig.6 Error of the results measured by the near-infrared binocular vision system**

Because the visible calibration board cannot be captured by NIRC, a calibration board with NIR-SMDs is designed, and the geometric information is measured by the visible binocular vision system. Then a calibration pattern with the geometric accuracy of up to 0.1320 mm is obtained, and it's independent of the measurement system. In order to calibrate the NIRC, the initial parameter values are obtained by DLT, and then more accurate parameters are achieved by the non-linear optimization method. In our experiments, the average relative errors of focal length and principal point of NIRC are 0.244% and 0.735%, respectively, the mean of image residuals is less than 0.01 pixel, and the 3D measurement error is less than 0.3 mm. These results indicate that the de-

signed calibration board and the used calibration method are reasonable. In short, the designed calibration board meets the requirement for calibrating the NIRC.

## References

- [1] L. Colace and G. Masini, *IEEE Journal of Quantum Electronics* **43**, 311 (2007).
- [2] X. Rang, Y. Huang and F. Gao, A Simple Camera Calibration Method based on Sub-Pixel Corner Extraction of the Chessboard Image, *IEEE Conference on Intelligent Computing and Intelligent Systems*, 688 (2010).
- [3] R. Y. Tsai, *IEEE Journal on Robotics and Automation* **3**, 324 (1987).
- [4] Z. Yan-Zhen and O. Zhou-Ying, *Journal of Image and Graphics* **16**, 1(2001).
- [5] Z. Zhang, *IEEE Transactions on Pattern Analysis and Machine Intelligence* **22**, 1330 (2000).
- [6] R. Wang and J. Guang, *Machine Vision and Application* **23**, 579 (2012).
- [7] X. Chen and J. Xi, *Optics and Lasers in Engineering* **47**, 310 (2009).
- [8] J. NIE, Z. MA and Y. HU, *Journal of Optoelectronics • Laser* **22**, 1826 (2011). (in Chinese)
- [9] R. Yang and C. Chen, *Optics and Lasers in Engineering* **46**, 373 (2008).
- [10] R. Yang, W. Yang, C. Chen and X. Wu, *Journal of Lightwave Technology* **29**, 3797 (2011).
- [11] R. Yang and Y. Chen, *IEEE Transactions on Instrumentation and Measurement* **60**, 608 (2011).
- [12] Jorge J. Moré, *Numerical Analysis* **630**, 105 (1997).
- [13] J. Draréni, R. Sébastien and P. Sturm, *International Journal of Computer Vision* **91**, 146 (2011).
- [14] Luis Puig, Yalin Bastanlar and Peter Sturm, *Journal of Computer Vision* **93**, 101 (2011).
- [15] Z. Wang, R. Yang, S. Liu, D. Xiong and X. Wu, *Journal of Optoelectronics • Laser* **23**, 203 (2012). (in Chinese)